

The buckling transition of 2D elastic honeycombs: Numerical simulation and Landau theory

E. A. Jagla

*The Abdus Salam International Centre for Theoretical Physics
Strada Costiera 11, (34014) Trieste, Italy*

I study the buckling transition under compression of a two-dimensional, hexagonal, regular elastic honeycomb. Under isotropic compression, the system buckles to a configuration consisting of a unit cell containing four of the original hexagons. This buckling pattern preserves the sixfold rotational symmetry of the original lattice but is chiral, and can be described as a combination of three different elemental distortions in directions rotated $2\pi/3$ from each other. Non-isotropic compression may induce patterns consisting in a single elemental distortion or a superposition of two of them. The numerical results compare very well with the outcome of a Landau theory of second order phase transitions.

I. INTRODUCTION

A two dimensional honeycomb structure formed by solid walls is the prototype of a cellular solid [1]. These are materials widely used in applications due to their remarkable mechanical properties, for instance its capacity for energy absorption under impact, and its low weight. Energy absorption is related to plastic deformation under stress. But still the ideally elastic and perfectly uniform two dimensional honeycomb presents some not completely solved puzzles. Under compressive stress, it has a buckling transition in which some (or all) of their walls bend. This transition is reminiscent of the well known buckling transition of an elastic bar under compressive stress at its extremes [2]. There has been some controversy on what the buckling mode of a regular honeycomb should be. On one hand, in their original work [3], Gibson and Ashby presented the results of an experiment using an elastomeric honeycomb, under what they called biaxial loading, in which they observed a non-trivial buckling pattern consistent with a symmetry breaking in which four original cells form the new repetitive motif of the material. In a posterior paper [4], Hutzler and Weaire performed numerical simulations and did not observe this pattern, but instead a buckling mode equivalent to that obtained under uniaxial stress. They argue that the pattern observed in Ref. [3] was a consequence of finite size effect, and the use of flat confining walls. Numerical results taking into account these effects [5] did show the pattern observed by Gibson and Ashby. Very recently, Okomura, Ohno and Noguchi [6] have studied the problem using a combination of a homogenization technique and finite elements numerical simulations. Their results do not agree with those of Hutzler and Weaire [4]. Instead, they found buckling patterns that can be interpreted as a superposition of three individual buckling modes. They also found that whether one, two, or three of these modes are active depends on the degree of anisotropy of the externally applied strain.

In view of the aforementioned contradiction between

[4] and [6], and considering that the techniques employed in both cases are quite different, an independent investigation to determine which of the two results is correct seems appropriate. In the first (numerical) part of this paper I will show that appropriately done numerical simulations using the technique used in [4] do not support the results claimed there, but instead those reported in [6]. In the second (more theoretical) part I will show how the results obtained in the simulations are fully compatible with the predictions of a Landau theory of second order phase transition applied to the buckling problem. This theory allows to obtain at once the buckled configuration of the system under a generic form of the macroscopically homogeneous applied deformation.

II. NUMERICAL SIMULATION

I have simulated a two dimensional honeycomb through the technique used in Refs. [4], [5], namely by considering the honeycomb walls as one dimensional rods, and including stretching and bending energy as

$$\begin{aligned} E_{stretch} &= \frac{1}{2}k_s \int \left(\frac{dl}{dl_0} - 1 \right)^2 dl_0 \\ E_{bend} &= \frac{1}{2}k_b \int c^2 dl_0 \end{aligned} \quad (1)$$

where c is the local curvature. To discretize these expressions I have used 7 intermediate points between any two neighbor vertices, but particular cases were checked using 18 points, to guarantee the absence of noticeable effects due to discretization. The only essential parameter of the model is k_b/L^2k_s , where L is the length of the individual rods. This ratio is physically related to the fraction Λ of two dimensional space that is occupied by the rods [1,4], namely $\Lambda = 4\sqrt{k_b/L^2k_s}$. The simulations presented below were done at $k_b/L^2k_s = 4.5 \times 10^{-4}$ (then $\Lambda = 0.085$), but additional checks indicate that the results are not qualitatively dependent on the precise

value of the parameter. All previously obtained buckling patterns for perfect honeycombs can be accommodated within a 2×4 unit cell. Then the elemental cell I simulated is precisely the 2×4 cell shown in Fig. 1(a), with periodic boundary conditions. The simulation method consists in calculating the forces acting on all points of the discretized system, and updating their positions using a viscous dynamics. The control variable was the macroscopic strain, that can be changed varying the size and shape of the simulation box. Stresses in the system can be evaluated both by numerical differentiation of the total energy with respect to strain, and by direct summation in terms of the forces between particles. The equivalence of the two results allows to check for consistency and convergence of the simulation.

Before indicating the results obtained, it is clarifying to discuss qualitatively the behavior observed (see [6]). The buckling structures that appear are related to reaccommodation of the vertices of the honeycomb structure, in such a way that lines of vertices forming zig-zag chains shift relatively to neighbor chains, as qualitatively indicated in Fig. 1(b). There are three of these modes, that will be referred to as the elementary modes of buckling. The patterns they generate will be called the uniaxial patterns. They are characterized by the unitary vectors shown in Fig. 1(e). Whether one, two, or the three elementary modes acquire non-zero amplitude at the buckling transition depends on the macroscopic strain applied. The qualitative pictures of Fig. 1(c) and (d) show the effect of combining two or three elementary modes. We see that the patterns of Fig. 1(b) and (c) are identical (except for the wall bending, that in this qualitative picture is not taken into account) to the patterns in Ref. [3]. The pattern in Fig. 1(c) will be referred to as the Gibson-Ashby pattern. The pattern in Fig. 1(d), that combines the three elementary modes, preserves the hexagonal symmetry of the structure (this will be referred to as the symmetric pattern). A buckling mode of this symmetry has been observed and simulated in [7], but only in the case of *plastic* buckling. To my knowledge, the only prediction of this mode for a perfectly elastic honeycomb is contained in [6]. It is remarkable that this pattern has lost the mirror symmetry plane of the original structure: it is a chiral pattern. The chirality can be defined as the sign of the product of the amplitudes of the three elementary modes from which the pattern is constructed.

In the numerical simulations, starting from the unstrained structure and isotropically compressing it, I have observed that the symmetric pattern is the stable configuration after buckling. However, it has to be mentioned that the transition from the unbuckled to the symmetrically buckled configuration, although continuous (then implying no surmounting of any energy barrier) may take a long computational time, and that other patterns (which correspond to saddles of the energy) can be

transitory observed. For instance, I show in Fig. 2 the mechanical energy of the system as a function of the compressive strain s in a single run increasing s at a constant rate. At the buckling point (at $s \simeq 0.0037$, note that I define s as $s = (s_x + s_y)/2$), and in the particular run shown, the system seems to buckle to the Gibson-Ashby pattern shown in Fig 3(b). This is not a minimum but a saddle of the energy, however it lasts long enough, and the energy of this branch can be numerically followed (as seen in Fig. 2 with open triangles) up to some strain at which it is observed to transform to the real energy minimum which corresponds to the symmetric pattern. In fact, when preparing the system in the symmetric pattern for large strain, and upon reduction of the strain, we obtain the results indicated by full circles in Fig. 2, which correspond to the real energy minimum of the system. In addition, if the system is prepared in the uniaxial or in the Gibson-Ashby pattern at large strain, and strain is reduced (sufficiently rapidly for the configuration not to destabilize, and sufficiently slowly so as energy can be calculated accurately) we can follow the energy of these two configurations, as indicated by the stars, and the full triangles in Fig. 2.

The uniaxial and Gibson-Ashby patterns may become the stable buckling modes under appropriate non-isotropic loading. For instance, by compressing along the x (y) direction, and keeping the perpendicular direction unstrained, I have observed the Gibson-Ashby (uniaxial) pattern to be stable after buckling. The stability of the Gibson Ashby pattern under particular uniaxial loading agrees again with the results in [6], but not with those claimed in [4]. We will see now how all these results can be fully systematized within a theoretical framework.

III. LANDAU THEORY OF THE BUCKLING TRANSITION

The results presented in the previous section are enough numerical input to construct the Landau theory of this peculiar second order transition. In fact, we see in Fig. 2 that the energies of all buckled configurations (whether the true minimum or the saddles) meet together in value and derivative at the buckling point, coinciding also at that point in value and derivative with the branch corresponding to the unbuckled system. This means that at the buckling point, in a generic parameter space, the state point of the system passes from a configuration with a single minimum (for the unbuckled state) to one with different minima and saddles in a continuous manner.

I will present a Landau description in which the order parameters are the three (small) amplitudes ϕ_1 , ϕ_2 , ϕ_3 of the elementary modes. For convenience, these three modes will be associated with the unitary vectors \mathbf{v}^1 , \mathbf{v}^2 , and \mathbf{v}^3 shown in Fig. 1(e). The free energy of the system (in the present case it actually corresponds simply to the

elastic energy) must a scalar, and then it can only contain combinations of the amplitudes and the (eventually anisotropic) external strains that are invariant with respect to the symmetry operations of the lattice. Considering for the moment only the isotropically compressed case, we should look for invariant combinations of the amplitudes. Up to fourth order those available are:

$$\begin{aligned} & \phi_1^2 + \phi_2^2 + \phi_3^2 \\ & (\phi_1^2 + \phi_2^2 + \phi_3^2)^2 \\ & \phi_1^2\phi_2^2 + \phi_2^2\phi_3^2 + \phi_3^2\phi_1^2 \end{aligned} \quad (2)$$

Then in this case the most general form of the free energy describing a second order transition is

$$F = \alpha(s_c - s)(\phi_1^2 + \phi_2^2 + \phi_3^2) + \beta(\phi_1^2 + \phi_2^2 + \phi_3^2)^2 - \gamma(\phi_1^2\phi_2^2 + \phi_2^2\phi_3^2 + \phi_3^2\phi_1^2) \quad (3)$$

with numerical constants α , β , and γ . This free energy has a single minimum at $\phi_p = 0$ ($p = 1, 2, 3$) for $s < s_c$, representing the unbuckled state. For $s > s_c$, this expression has saddles (or minima) at the following values of the amplitudes:

$$\phi_p^2 = A, \quad \phi_q = 0, \quad \phi_r = 0 \quad (4)$$

$$\phi_p^2 = B, \quad \phi_q = B, \quad \phi_r = 0 \quad (5)$$

$$\phi_p^2 = C, \quad \phi_q = C, \quad \phi_r = C \quad (6)$$

where p, q, r are arbitrary permutations of 1, 2, 3, and A, B, C , are given by:

$$A = \frac{(s - s_c)\alpha}{2\beta} \quad (7)$$

$$B = \frac{(s - s_c)\alpha}{4\beta - \gamma} \quad (8)$$

$$C = \frac{(s - s_c)\alpha}{6\beta - 2\gamma} \quad (9)$$

They correspond respectively to the uniaxial, Gibson-Ashby, and symmetric patterns. The corresponding values of the free energy are,

$$f_{uni} - f_{unb} = -\frac{(s_c - s)^2\alpha^2}{4\beta} \quad (10)$$

$$f_{GA} - f_{unb} = -\frac{(s_c - s)^2\alpha^2}{4\beta - \gamma} \quad (11)$$

$$f_{sym} - f_{unb} = -\frac{(s_c - s)^2\alpha^2}{4\beta - 4\gamma/3} \quad (12)$$

(I have subtracted the free energy of the unbuckled system f_{unb} , that is taken as zero in the Landau theory, but that should be included when comparing with the results of the numerical simulations). We see that the symmetric pattern is the minimum energy one for $\gamma > 0$ (whereas the uniaxial pattern provides the absolute minimum if

$\gamma < 0$). Then, in order to agree with the simulation results, we will assume $\gamma > 0$. The physical justification for the positive sign of γ is not provided by the Landau theory, and should come from an explicit evaluation of the mechanical energy of the honeycomb. From the previous values of the free energy a parameter free relation can be obtained and compared with the numerical results. First note that the ratio β/γ can be obtained for instance as

$$\frac{\gamma}{\beta} = 3 \left(\frac{f_{sym} - f_{uni}}{f_{sym} - f_{unb}} \right) \quad (13)$$

This in particular should be independent of the actual value of the compression s (as long as $s > s_c$). From the numerical results it can be obtained that this ratio is in fact independent on s , and the numerical value is approximately $\gamma/\beta \simeq 0.01$ for the parameters of the simulation. Then note that to a very good approximation we have

$$\frac{f_{GA} - f_{sym}}{f_{uni} - f_{sym}} = \frac{1}{3} \quad (14)$$

This is a parameter free relation that has to be satisfied in our numerical simulations. From the data in Fig. 2, it can be in fact verified that this is very accurately satisfied. This is a strong evidence that the present Landau theory describes the physics of the present buckling transition.

In order to make the theory more complete, I want to consider now the possibility of non-isotropic external loading on the system. This means that instead of a single parameter s , we have now a generic (symmetric) strain tensor s_{ij} ($i, j = 1, 2$) applied onto the system (the previously introduced isotropic compression s is related to the trace of this tensor). This has to be introduced into the free energy in a symmetrically invariant form. To lowest order I will include it only in the second order term, which is the one that triggers the transition. Using the unitary vectors $\mathbf{v}^1, \mathbf{v}^2, \mathbf{v}^3$ of the elementary modes, two different terms quadratic in the amplitudes can be written:

$$F^{(1)} \sim \sum_{i,j=1,2} \sum_{p,q=1,2,3} s_{ij} v_i^p v_j^q a_{pq} \phi_p \phi_q \quad (15)$$

$$F^{(2)} \sim \sum_{i,j=1,2} \sum_{p,q=1,2,3} s_{ij} v_i^p v_j^q b_{pq} \phi_p \phi_q \quad (16)$$

where a_{pq} and b_{pq} are arbitrary numeric matrices. However, these expressions have to be invariant under permutation of the elementary vectors (since this is a symmetry operation obtained by the mirror symmetry along the line containing the third vector) and sign change of any of the amplitudes (which is obtained by a particular spatial translation allowed by symmetry). Then it is obtained that both a_{pq} and b_{pq} matrices should be proportional to the identity, i.e.,

$$F^{(1)} \sim \sum_{i,j=1,2} \sum_{p=1,2,3} s_{ii} v_i^p v_i^p \phi_p^2 \quad (17)$$

$$F^{(2)} \sim \sum_{i,j=1,2} \sum_{p=1,2,3} s_{ij} v_i^p v_j^p \phi_p^2 \quad (18)$$

Then $F^{(1)}$ becomes proportional to $s_{ii}(\phi_1^2 + \phi_2^2 + \phi_3^2)$ and is the term considered in the isotropically compressed case.

To analyze the second contribution it can be more convenient to use the following definition of the three independent components of the strain tensor:

$$\begin{aligned} s &= (s_{11} + s_{22})/2 \\ s_2 &= (s_{11} - s_{22})/2 \\ s_3 &= s_{12} = s_{21} \end{aligned}$$

which represent the applied deformation in a more physical way: s represents an isotropic compression (we already used this), whereas s_2 and s_3 are the two independent shear modes, which are related by a $\pi/4$ rotation. In terms of these variables, and using explicitly the components of the unitary vectors we finally arrive to the following form of the free energy:

$$\begin{aligned} F &= \alpha [(s_c - s)(\phi_1^2 + \phi_2^2 + \phi_3^2)] + \\ &+ \delta \left[s_2 (\phi_1^2 - \phi_2^2/2 - \phi_3^2/2) + s_3 \frac{\sqrt{3}}{2} (\phi_3^2 - \phi_2^2) \right] + \\ &+ \beta (\phi_1^2 + \phi_2^2 + \phi_3^2)^2 - \gamma (\phi_1^2 \phi_2^2 + \phi_2^2 \phi_3^2 + \phi_3^2 \phi_1^2) \quad (19) \end{aligned}$$

This is the final expression for the free energy close to the buckling transition. Minimizing it we can obtain the buckled state under any particular combination of the three independent strains s , s_2 , and s_3 . Note that as this expression has to describe also the unstrained system, and then αs_c and δ will be respectively proportional to bulk and shear modulus of the original structure, then typically $\delta \ll \alpha s_c$.

I want to describe now the buckling mode map of the system, namely, what the amplitudes of the three elementary modes are for any choice of the strain tensor. First notice the following scaling of the free energy: If we consider the values of the three order parameters at the minimum of (19), namely ϕ_{min}^p , to be a function of $s_c - s$, s_2 , and s_3 , then the following relation is satisfied:

$$\phi_{min}^p(s_c - s, s_2, s_3) = \lambda^{-1/2} \phi_{min}^p(\lambda(s_c - s), \lambda s_2, \lambda s_3) \quad (20)$$

This implies in particular that the borders between different regions in the parameters space $s_c - s$, s_2 , and s_3 are spanned by rays propagating from the origin.

I will analyze a couple of particular cases. First consider the case $s_3 = 0$, i.e., purely compressive strains along x and y (although non necessarily equal). I show in Fig. 4(a) the map of buckling modes in the s - s_2 plane

for this case. The borders between different regions can be worked out analytically. All of them are straight lines emanating from the point $s = s_c$, $s_2 = 0$, as the previous argument indicates. The transition between unbuckled ($\phi_p \equiv 0$) and uniaxial pattern ($\phi_1 \neq 0$) can be easily obtained setting $\phi_2 = \phi_3 = 0$ in (19). The limit line is given by $s_2 = (s - s_c)\alpha/\delta$. The transition line between the unbuckled and the Gibson-Ashby pattern ($\phi_2 = \phi_3 \neq 0$) is obtained along the same lines, as $s_2 = -2(s - s_c)\alpha/\delta$. Increasing s at $s_2 = 0$, the symmetric pattern appears at $s = s_c$, as we already know from the isotropically compressed case. The symmetric pattern loses its strict rotational symmetry for any $s_2 \neq 0$. However, it still has the three elementary model active as long as we are within the V-shaped region in Fig. 4(a). The limits of this region are given by

$$s_2^{(uni \rightarrow sym)} = \frac{1}{3} \frac{\alpha \gamma}{\beta \delta} \frac{s_c - s}{\left(1 - \frac{\gamma}{3\beta}\right)} \quad (21)$$

for the transition to the uniaxial pattern, and

$$s_2^{(GA \rightarrow sym)} = -\frac{1}{6} \frac{\alpha \gamma}{\beta \delta} \frac{s_c - s}{\left(1 - \frac{\gamma}{3\beta}\right)} \quad (22)$$

for the transition to the Gibson-Ashby pattern. Note the exact relation

$$s_2^{(GA \rightarrow sym)} / s_2^{(uni \rightarrow sym)} = -2 \quad (23)$$

valid for any values of the parameters of the free energy.

The results of Fig. 4(a) are fully compatible with the results in [6] (in particular, relation (23) is very well satisfied). We note that for the present parameters the stability of the single elementary mode and Gibson-Ashby pattern that was obtain numerically under uniaxial compression is recovered.

As an additional example I show the map of buckling modes in the s_2 - s_3 plane for some $s > s_c$ in Fig. 4(b). Note the nice symmetry of this pattern, which has one two or three elementary modes active depending on the particular choice of the applied strains s_2 and s_3 (remember that s_2 and s_3 are related by a rotation of $\pi/4$). Again, all borders between different sectors are straight lines. The analytical expression for the line separating sectors 1 and 1,2 is given by

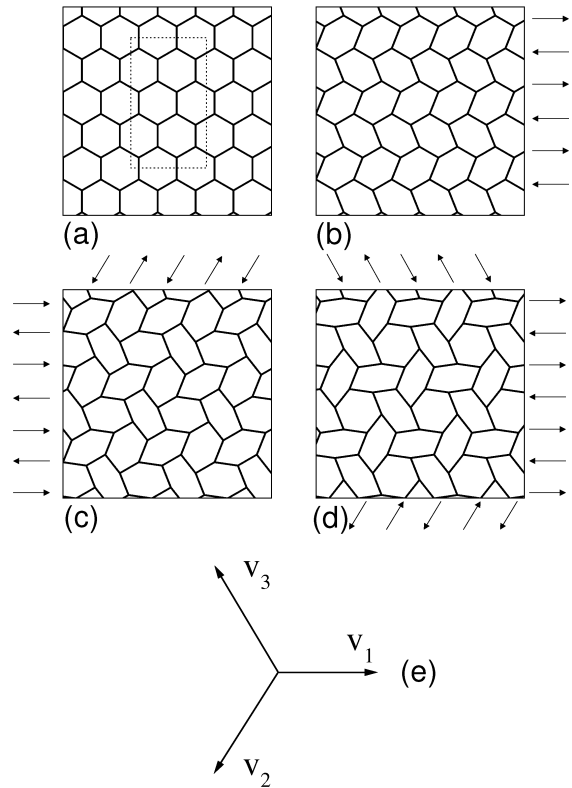
$$s_3 = \sqrt{3} s_2 \left(1 - \frac{\gamma}{3\beta}\right) - \frac{\alpha \gamma}{\sqrt{3} \beta \delta} (s_c - s) \quad (24)$$

All other lines can be obtained then from symmetry.

To finish, we note that all transitions in the parameter space are continuous, namely, there are no jumps of the order parameters at any point, and there is no possibility of metastabilities either.

IV. CONCLUSIONS

The buckling mode of an elastic two dimensional honeycomb provides an example of non-trivial patterns with symmetry breaking appearing in a very simple mechanical system. Remarkably, for isotropic compression the symmetry breaking produces the appearance of a chiral ground state. This problem is also a realization of a second order transition that can be accurately modeled through a Landau theory constructed on the basis of the symmetry of the problem. The agreement between the Landau theory and the numerical simulation is seen to be very good.



-
- [1] Gibson L J and Ashby M F 1988 *Cellular Solids: Structure and Properties* (Oxford: Pergamon)
 - [2] Timoshenko S P and Gear J P 1961 *Theory of Elastic Stability* (Mac Graw Hill-Tokio)
 - [3] Gibson L J and Ashby M F, Ref. [1], page 99.
 - [4] Hutzler S and Weaire D 1997 *J. Phys.: Condens. Matter* **9** L323
 - [5] Hutzler S and Weaire D 1999 *The Physics of Foams* (Oxford, Clarendon)
 - [6] Ohno N, Okumura D and Noguchi H 2002 *J. Mech. Phys. Solids* **50** 1125
Okumura D, Ohno N and Noguchi H 2002 *Int. J. Solids Struct.* **39** 3487
 - [7] Papka S D and Kyriakides S 1999 *Int. J. Solids Struct.* **36** 4367
Papka S D and Kyriakides S 1999 **36** 4397

FIG. 1. (a) The hexagonal starting lattice. Dotted box is the system actually simulated. (b) Upon shifts of the vertices as indicated by the arrows, the uniaxial pattern is obtained. Note however that there are three equivalent ways of generating this pattern, that can be characterized by the unitary vectors shown in (e). Combining two or the three of them we obtain the configurations in (c) and (d).

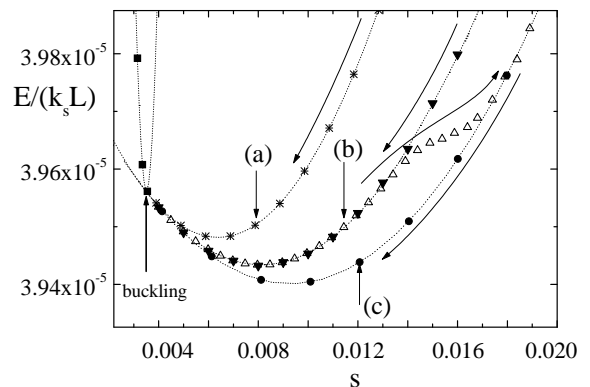


FIG. 2. Total energy of the simulated system (dotted box in Fig. 1(a)) as a function of compressive strain $s \equiv (s_x + s_y)/2$. A global, linear contribution in s has been subtracted to appreciate tiny differences in energy. All continuous lines are quadratic fitting of the data close to the buckling point. Results are shown from a running from the unbuckled state (squares), in which a Gibson-Ashby pattern is generated first (open triangles). This is however a saddle of the energy, and is seen to transform to the symmetric pattern after some time. The other three curves show the results starting from the uniaxial (stars), Gibson-Ashby (full triangles), and symmetric (circles) patterns at high strain, and reducing it towards the unstrained configuration. Note how the minimum energy of the buckled state is obtained for the symmetric pattern. The letters indicate where the snapshots in Fig. 3 were taken.

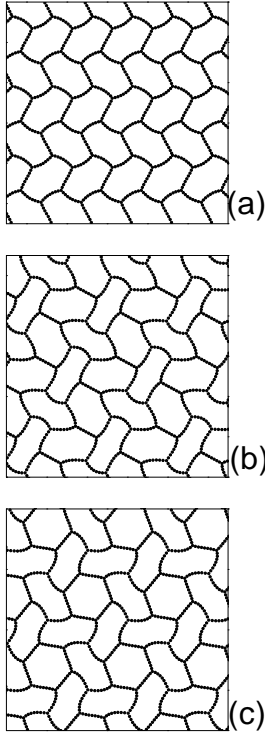


FIG. 3. The uniaxial, Gibson-Ashby, and symmetric buckling modes. The snapshots correspond to the points indicated in Fig. 2. For isotropic compression, the symmetric pattern provides the minimum energy, the other two correspond to saddles, and eventually destabilize. However, they can be made stable under appropriate non-isotropic loading (the displacements with respect to the hexagonal configuration have been amplified by a factor of 5 to render the geometrical structure more visible).

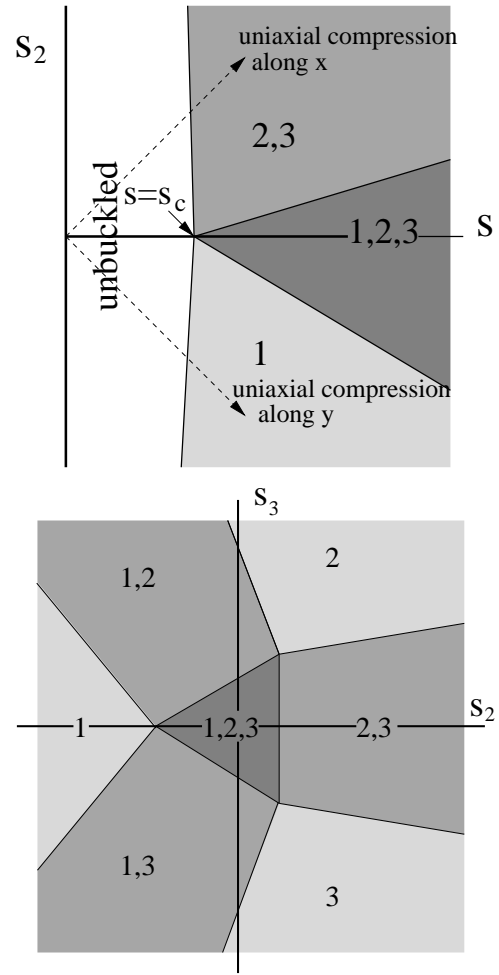


FIG. 4. The buckling modes map in the s - s_2 plane for $s_3 = 0$ (a), and in the s_2 - s_3 plane for a constant value of $s > s_c$ (b). In each region, the numbers indicate which elementary modes are active (see Fig. 1). The analytical expressions for the limits between different regions are given in the text.